REVISTA INTERDISCIPLINAR DE PESQUISA EM ENGENHARIA

CILAMCE 2016

XXXVII IBERIAN LATIN AMERICAN CONGRESS ON COMPUTATIONAL METHODS IN ENGINEERING
BRASÍLIA - DF - BRAZIL

A CRITICAL ASSESSMENT OF PHENOMENOLOGICAL MODELS UNCERTAINTIES FOR TURBIDITY CURRENTS

Henrique José Ferreira da Costa

Fernando Alves Rochinha

hefecosta@gmail.com

faro@mecanica.coppe.ufrj.br

COPPE-UFRJ Universidade Federal do Rio de Janeiro

Centro de Tecnologia - Av. Horácio Macedo, 2030, Rio de Janeiro - RJ - Brasil, 21941-450

Abstract. *Turbidity currents have significantly contributed to the formation of oil reservoirs through massive transport and deposition of sediments in the offshore area during the past geological era. That motivates the seek for understanding these complex flows composed of carrier and disperse phases. In this regard, numerical simulations can be of great help in understanding the complex underlying physics of those turbulent flows. Two-fluid models allow the explicit consideration of both phases, liquid and solid, where the coupling between them arises from fluid-particle and particle-particle interactions. Simplified approaches, namely standard sediment transport model (SSTM) and partial two-fluid model (PTFM), represent a balance between accuracy and easiness of computation which makes them attractive for different applications. Computational models are built upon employing a Large Eddy Simulation (LES) approach based on the Residual Based Variational Multiscale Method (RBVMS). The scales decomposition used in the RBVMS allow the design of subgrid models, responsible for describing turbulence and interactions involving fine scales that are not captured by the numerical grid, on a purely computational modeling standpoint. Using those computational models on an uncertainty quantification perspective, a number of simulations are performed aiming at assessing the role of phenomenological models as surrogates for the two-fluid models direct interactions in nondilute flows. Uncertainties of those models are embedded into random parameters variables. Different scenarios involving an open channel flow were performed to make a critical analysis of those submodels when applied to turbidity currents simulations.*

Keywords: *Reduced Model, Uncertainty Quantification, Turbidity Current*

1 INTRODUCTION

Turbidity currents are composed of a fluid and solid particles, called sediments. These flows are most commonly evaluated in the oil and gas industry where they are considered to be the main responsible for the formation of oil reservoirs due to the deposition, providing sedimentary reservoirs.

The complexity of these flows is due to the presence and coupling of several phases, each one with its characteristic flows. The presented model to simulate turbidity currents considers water and sediment, each one with its governing equations, built after two-fluid model approach. The coupling between them should be considered, particularly when the concentration increases. To achieve a good prediction of the concentration and velocities profile, the coupling, fluid-particle and particle-particle as well, have been considered by the inclusion of interaction forces and phenomenological models associating the viscosity with the concentration.

However, the phenomenological models for rheology of these currents provide a source of uncertainty due to their plurality in literature and their own different parameters may be considered uncertain. So a discussion of an application of a stochastic colocation approach on these models will be presented.

This article is divided as follows in section 2 the different phenomenological equations for rheology are described, in the section 3, the mathematical formulation and in section 4, some results and discussions.

2 PHENOMENOLOGICAL EQUATIONS

Einstein (1906) realizes that in turbidity currents the classic approach of considering the constant viscosity for this mixture overestimates the system global energy. He proposes several ways to deal with it. One is to consider the particles diffusivity in the mass balance of the sediment, represented in the Eq. (1), so, the diffusion coefficient, D_s, is

$$D_s = \frac{\kappa}{T} 6\pi\mu d_p \tag{1}$$

where κ is the Boltzmann constant, T, the temperature, μ, the water viscosity, and d_p, the diameter of the sediment. However, when referring to the mixture flow as a whole, Einstein (1906) derived the equation (2). Taking into account the linear momentum balance, he achieves in this expression of viscosity in function of the particle concentration,

$$\mu_m = \mu\left(1 + 2.5C\right) \tag{2}$$

where μ_m is the viscosity of the mixture water-sediment. In his analysis, he made some assumptions: there is no interaction between particles, the particles are spherical and concentrations are up to 0.05 %. Following his steps, several authors have worked to expand the accuracy and application of this equation. Batchelor (1977) employs probabilistic models and found the Eq. (3), a second-degree equation to express the viscosity in function of sediment concentration

$$\mu_m = \mu\left(1 + 2.5C + 6.2c^2\right) \tag{3}$$

achieving good results, according to the author, when compared with experimental observations with concentrations up to 30 %.

There are several other equations, each one with its analysis. Arrhenius (1917) assumes that the dependence of the viscosity in relation to the concentration is exponential and showed that experimental observations prove his inference. Among the different approaches evaluated in this study and summarized in Table 1, it has to be point out the existence of two parameters: the exponential factor and the maximum packing fraction.

Table 1: Different viscosity equations depending on the concentration, taken from Widera (2011).

Author	Equation
Einstein (1906)	$\mu_m = \mu\left(1 + 2.5C\right)$
Mooney (1951)	$\mu_m = \mu\left[\exp\left(\frac{2.5C}{1-\frac{C}{C_m}}\right)\right]$
Roscoe (2002)	$\mu_m = \mu\left[1 - \frac{C}{C_m}\right]^{-2.5}$
Krieger & Dougherty (1959)	$\mu_m = \mu\left[1 - \frac{C}{C_m}\right]^{-2.5C_m}, C_m = 0.74$
Thomas (1965)	$\mu_m = \mu[1 + 2.5c + 10.05C^2$ $0.00273 + \exp(16.6C)]$
Chong *et al.* (1971)	$\mu_m = \mu\left[1 + \frac{0.75\frac{C}{C_m}}{1-\frac{C}{C_m}}\right]; C_m = 0.55$
Batchelor (1977)	$\mu_m = \mu\left[1 + 2.5C + 6.2C^2\right]$
Brady (1993)	$\mu_m = 1.3\mu\left[1 - \frac{C}{C_m}\right]^{-2.0}$
Toda & Furuse (2006)	$\mu_m = \mu\left[\frac{1-0.5C}{(1-C)^3}\right]$
Toda & Furuse (2006)	$\mu_m = \mu\left[\frac{1+0.5kC-C^2}{(1-kC)^2(1c)}\right]\ k + 1 = 0.6C$

Then, the viscosity is shown to be a function of sediment concentration using only these two parameters. Moreover, Pavlik (2011) shows through his experiments that the determination of these parameters is neither simple nor deterministic. Through regression of experimental observations in a circular viscometer, he determined bounds for these parameters.

Taking into consideration which seems to be the most characteristic equation for both its simplicity and concepts, we choose Krieger & Dougherty (1959)'s expression, Eq. (4), in order to perform our analysis on rheology,

$$\mu_m = \mu\left[1 - \frac{C}{C_{max}}\right]^{-\lambda C_{max}} \tag{4}$$

The maximum concentration C_{max} imposes that the viscosity of the mixture has an asymptote when the concentration reaches this value. The exponential parameter λ brings an adjustment to the exponential curve. For the authors, $\lambda = 2.5$, which respects the Einstein's equation for small concentrations.

In order to visualize the model discrepancy of Table 1, Fig. 1 shows the efect of λ parameter embeded in this phenomenological equation. As Krieger & Dougherty (1959) apply the equation for concentrations up to 60 %, and according to Pavlik (2011) results, we consider a variation of λ. Fig. 1 shows that a dispersion of λ in the equation of Krieger & Dougherty

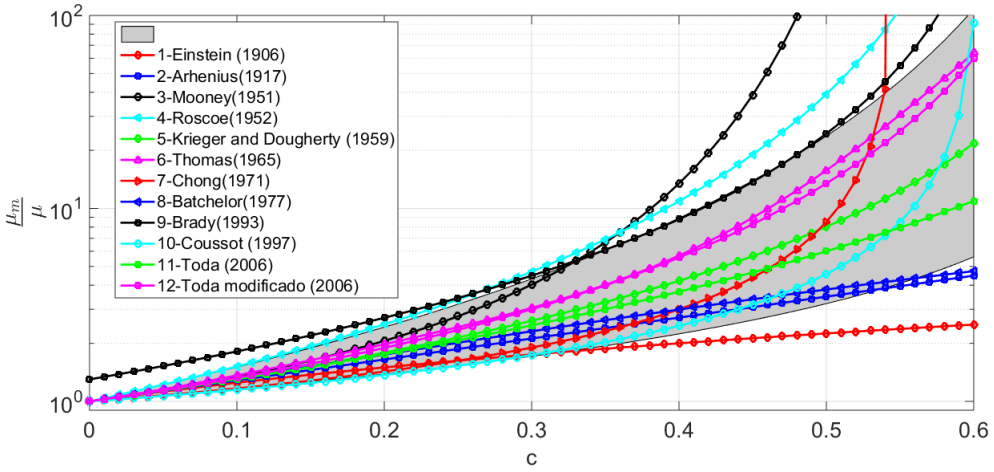

Figure 1: visual shows the influence of the parameter λ of the equation of Krieger & Dougherty (1959), such that $1.4 \leq \lambda \leq 3.8$

(1959), such that $1.4 \leq \lambda \leq 3.8$, is able to capture almost all the other phenomenological equations of Table 1. It has to be noticed that, this plot extrapolates the range of application of some equations, for example, Einstein's equation that is valid only for concentrations smaller than 0.05 %. In this regard, it is noteworthy that the viscosity curves that are outside the gray area at the bottom right of the figure are out of their range of application. Thus, we are able to embed the model uncertainty with a parameter analysis.

3 MATHEMATICAL FORMULATION

Jha & Bombardelli (2010), Jha & Bombardelli (2011), Bombardelli & Jha (2009), Buscaglia *et al.* (2002), Elghobashi (1983) among others made use of two fluid model formulation to simulate turbidite currents, where the volume concentration is associated to the probability of sediment in each element. Using the same idea, there is here an exploitation of two different formulations derived from the two-fluid model: the standard model, *Standard Sediment Transport Model* (SSTM), and the *Partial Two Fluid Model* (PTFM). This work aims to compare those models applying an uncertainty quantification approach on standard model in order to obtain the data of the partial two-fluid model, which considers more complex coupling and physic. The numerical modeling is based on the *Residual Based Variational Multiscale Method* (RBVMS) for dealing with the decomposition of scales and numerical stability.

3.1 Governing equations

The difficulty in the study of turbidity currents occurs essentially in the consideration of several kinds of interaction. When the concentration is low, they may be neglected. With higher concentrations, they could affect significantly the results. The two fluid model permits falling into the equations consideration not only of the fluid-particle interaction but also the particle-particle interaction forces. The proposed models consider a two-way coupling for the standard model (SSTM) and a more complete coupling, the partial two fluid model (PTFM). In addition to the viscosity depending on concentration which is considered by Widera (2011) as a better form of describing the coupling effects, we are able to point out these different forms of interaction: coupling from the phenomenological equations and consideration of the forces from the interaction between the particles.

3.2 General form of the two-fluid model

In two-fluid models, each fluid is considered as a phase. Therefore, the governing equations of the mass balance and the momentum balance for each phase k are the Eqs. (5) and (6) respectively. The mass balance considering mass transfer from one phase to the other, is represented by Γ_k

$$\frac{\partial \alpha_k \rho_k}{\partial t} + \nabla \cdot (\alpha_k \rho_k \mathbf{u}_k) = \Gamma_k \tag{5}$$

where α_k is the concentration and $\mathbf{u}_k$, the velocity of the phase k and ρ_k, the density of the phase k. The term Γ_k is considered to be the molecular effect of the particles, introducing diffusion into sediment movement, represented by a constant diffusion coefficient according to Eq. (1).

The other governing equation represents the momentum equilibrium, Eq. (6), or transport equation,

$$\frac{\partial \alpha_k \rho_k \mathbf{u}_k}{\partial t} + \nabla \cdot (\alpha_k \rho_k \mathbf{u}_k \otimes \mathbf{u}_k) = -\alpha_k \nabla p + \nabla \cdot \left[\mu_k \left(\nabla \mathbf{u}_k + \nabla \mathbf{u}_k^T\right)\right] + \alpha_k \rho_k \mathbf{b}_k + \mathbf{M}_k + \mathbf{U}_{ki} \Gamma_k \tag{6}$$

where p, $\mathbf{b}_k$, $\mathbf{M}_k$ and $\mathbf{U}_{ki}$ stands for the pressure, the terms of volumetric forces as gravity and forces of interaction between phase respectively. These last three terms represent the interaction forces between the different phases as interaction between particles. The viscosity μ_k is considered dependent on the concentration and comes from the phenomenological equation of Krieger and Dougherty. In order to preserve consistency between phases, mixing rules associate the variables of the various liquid-solid phases together expressed second Brennen (2005); Cao *et al.* (1995, 2003) in Eqs (7) (8), (10) and (9)

$$p = p_m = p_s = p_f \tag{7}$$

$$\alpha_s + \alpha_f = \alpha_m = 1 \tag{8}$$

$$\rho_m = \alpha_s \rho_s + \alpha_f \rho_f \tag{9}$$

$$\rho_m \mathbf{u}_m = \alpha_s \rho_s \mathbf{u}_s + \alpha_f \rho_f \mathbf{u}_f \tag{10}$$

where the subscripts m, s and f stands for the mixture, the sediment or the environmental fluid, p, pressure, α, the concentration, ρ, the density and $\mathbf{u}$, the velocity. This set of equations enables to apply the Eqs. (5) and (6) to the mixture and thus recover the form of the Navier-Stokes equations. That is the basis of the numerical framework dealed here.

3.3 Models derived from the two-fluid model

The PTFM considers the mixture as a phase and the sediment as another distinct phase. Meanwhile, the SSTM considers the momentum balance of the sediment equal to the mixture. It is possible to find the governing equations of mass and momentum balance for each phase in the respective models. Note that what is being called the mass balance of the sediment is not properly speaking, and this is due to the fact that the sediment has no independent kinematics.

Thus, associating the definition equations of the quantities of the mixture equations (7) (8), (10) and (9) with the governing equations (5) and (6) it stands the mixture mass and momentum balance equations (11) and (12) respectively. Adding the equations (13) and (14) for,

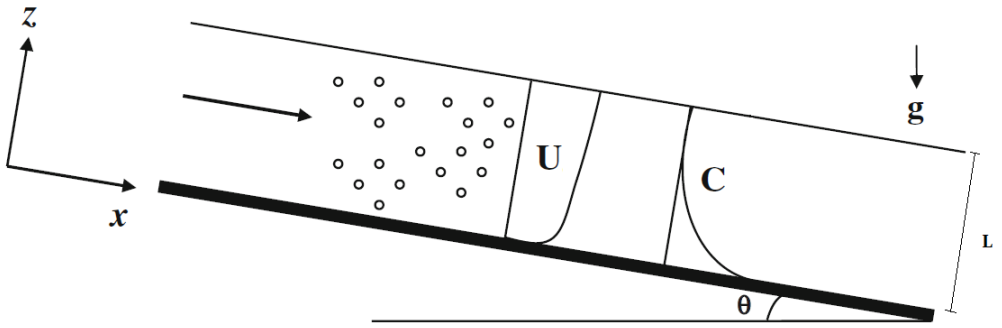

Figure 2: Domain illustration where the models have been developed

respectively, sediment mass and momentum balance, there is a system of governing equations for PTFM, representing a turbidity current,

$$\nabla \cdot (\mathbf{u}_m) = 0 \tag{11}$$

$$\frac{\partial \rho_0 \mathbf{u}_m}{\partial t} + \nabla \cdot (\rho_0 \mathbf{u}_m \otimes \mathbf{u}_m) = -\nabla p + \nabla \cdot \left[\mu_m \left(\nabla \mathbf{u}_m + \nabla \mathbf{u}_m^T\right)\right] + \rho_m \mathbf{g} \tag{12}$$

$$\frac{\partial \alpha_s \rho_s}{\partial t} + \nabla \cdot (\alpha_s \rho_s \mathbf{u}_s) = \nabla \cdot [D_s \cdot \nabla (\alpha_s \rho_s)] \tag{13}$$

$$\frac{\partial \alpha_s \rho_s \mathbf{u}_s}{\partial t} + \nabla \cdot (\alpha_s \rho_s \mathbf{u}_s \otimes \mathbf{u}_s) = -\alpha_s \nabla p + \nabla \cdot \left[\alpha_s \mu_s \left(\nabla \mathbf{u}_s + \nabla \mathbf{u}_s^T\right)\right] + \alpha_s \rho_s \mathbf{g} + \mathbf{M}_s \tag{14}$$

where the superscript T is the transposed matrix, $\mathbf{g}$, the gravitational acceleration vector and ρ_0, the reference density.

In order to have a more appropriate setup for analysis, a usually employed simplification in hydrology was carried out, following (Winterwerp, 2002), the so-called *" 1DV-POINTMODEL "*. This procedure has been used within two fluids models, such as in Bakhtyar *et al.* (2009); Bombardelli & Jha (2009). Therefore, the equations are developed for a bi- or tri-dimensional flow and the resolution occurs in a one-dimensional domain. Fig. 2 reproduces two dimensions flow analyzed. In this procedure, it is assumed that the derivatives due to x and y directions are approximately zero.

The flow tends to be fully developed over time, with the partial derivative of the speed function x being zero, which is used as an ending criterion for the simulation. Using capital letters for speed, W in z and U in x, and C for the sediment concentration, and developing the governing equations presented for a scenario of constant pressure, it leads to, for SSTM, a system of six equations: the mass balance of the mixture, Eq. (15) at the momentum equilibrium for mixing, in x, Eq. (16), and, in z, Eq. (17), the mass balance of the sediment, Eq. (18), the sediment momentum balance in x, Eq. (19) and in z, Eq. (20)

$$\frac{\partial W_m}{\partial z} = 0 \tag{15}$$

$$\frac{\partial \rho_0 U_m}{\partial t} = \frac{\partial}{\partial z}\left[\nu_m \frac{\partial \rho_0 U_m}{\partial z}\right] + \rho_m g S \tag{16}$$

$$W_m = 0 \tag{17}$$

$$\frac{\partial C}{\partial t} + W_s \frac{\partial C}{\partial z} = \frac{\partial}{\partial z}\left[D_s \frac{\partial C}{\partial z}\right] \tag{18}$$

$$U_s = U_m \tag{19}$$

$$W_s = -W_{set} \tag{20}$$

where ν is the kinematic viscosity and S the slope of the flow which is the sinus of the angle θ in Fig. 2.

The settling velocity W_{set} was considered constant. The density ρ_0 was considered as the density of the fluid. In this case, the coupling of the transport equations with the momentum equation takes into account only the gravity force where the density of the mixture is in function of concentration. The sediment momentum balance in the longitudinal direction of the flow is equal to the mixture since their velocities are equal. So there is a double coupling: the gravitational force and the viscosity depending on the concentration.

The same procedure applyed for PTFM also yields a set of six equations: the mixture mass balance, Eq. (21), the mixture momentum balance in x, Eq. (22), and in z, Eq. (23), the sediment mass balance, Eq. (24), the sediment momentum balance in x, Eq. (25), and in z, Eq. (20)

$$\frac{\partial W_m}{\partial z} = 0 \tag{21}$$

$$\frac{\partial \rho_0 U_m}{\partial t} = \frac{\partial}{\partial z}\left[nu_e ff, m\frac{\partial \rho_0 U_m}{\partial z}\right] + \rho_m g S \tag{22}$$

$$W_m = 0 \tag{23}$$

$$\frac{\partial C}{\partial t} + W_s \frac{\partial C}{\partial z} = \frac{\partial}{\partial z}\left[D_s \frac{\partial C}{\partial z}\right] \tag{24}$$

$$\frac{\partial C\rho_s U_s}{\partial t} + \frac{\partial C\rho_s U_s W_s}{\partial z} = \frac{\partial}{\partial z}\left[\nu_s \frac{\partial C\rho_s U_s}{\partial z}\right] + C\rho_s g S + F_{D,x} + F_{VM,x} + F_{L,x} \tag{25}$$

$$W_s = -W_{set} \tag{26}$$

where the quantities involved are analogous to SSTM, differing only in the fact that sediment velocity comes from the momentum balance equation, which, consequently, includes coupling forces. The fluid-particle coupling forces, as well as particle-particle coupling present in sediment momentum balance in x, Eq. (25) are represented in drag forces, Eq. (27), lift forces, Eq. (28), and virtual mass, Eq. (29) according to Dong & Zhang (1999); Bakhtyar *et al.* (2009); Bombardelli & Jha (2009),

$$F_{D,x} = \left[\frac{3}{4d_s} C\rho_m C_D \sqrt{(U_m - U_s)^2 + (W_m - W_s)^2}\right] \times (U_m - U_s) \tag{27}$$

$$F_L = x - C_L C \rho_m W_s \frac{\partial U_m}{\partial z} \tag{28}$$

$$F_{VM,x} = \frac{C\rho_m}{2}\left[\frac{\partial (U_m - U_s)}{\partial t} - W_s \frac{\partial U_s}{\partial z}\right] \tag{29}$$

where the drag coefficient, C_D, is found by the expression, equation (30), involving the explicit

particle Reynold number, Re_r, equation (31),

$$C_D = \frac{24}{Re_r}\left(1 + 0,15Re_r^{0,687}\right) \tag{30}$$

$$Re_r = \frac{\rho_f \left|U_f - U_s\right| d_s}{\mu} \tag{31}$$

and the lift coefficient, C_L is constant and equal to $4/3$, according to Bakhtyar *et al.* (2009); Bombardelli & Jha (2009).

Boundary conditions are Neumann type at the bottom and Dirichlet on the top. This way, the equation (32) and the no-slip condition, $U_m = U_s = 0$ are applyed at the bottom and the Eqs. (33) and (34), on the top.

$$D_s \left.\frac{\partial C}{\partial z}\right|_{z=0} = -\left. C\right|_{z=0} w_{set} \tag{32}$$

$$\frac{\partial U_m}{\partial z} = \frac{\partial U_s}{\partial z} = \frac{\partial U_f}{\partial z} = \frac{\partial W_s}{\partial z} = W_f = W_m = 0 \tag{33}$$

$$\left.\left(C w_{set} + D_s \frac{\partial C}{\partial z}\right)\right|_{z=h} = 0 \tag{34}$$

Thus, it maintains the physical conditions of the domain boundary. For consideration of the inherent turbulence to turbidity currents due to the density difference between phases the scale decomposition method of *Residual Based Variational Multiscale Method* (RBVMS) employed with finite element method will be used, as in Guerra *et al.* (2013); Avila *et al.* (2015); Bauer *et al.* (2012).

3.4 Formulation RBVMS

The RBVMS consists in a variable decomposition in coarse and fine scales. A Large Eddy Simulation (LES) grid is the base for considering the fines scales which bring stability and turbulent consideration. The subgrid values are calculated from the respective residua of the governing equations (Guerra *et al.* , 2013; Avila *et al.* , 2015; Bauer *et al.* , 2012). The equations (35) (36) and (37) formally introduce this decomposition, taking into account the quantities of the coarse grid, with subscript h, and the quantities from the subgrid with an apostrophe:

$$C = C^C H + C' \tag{35}$$

$$U_m = U_m^h + U_m' \tag{36}$$

$$U_s = U_s^h + U_s' \tag{37}$$

where the quantities of fine scales are modeled numerically according to a stabilization term and the residua of the corresponding governing equation as shown in the Eqs. (38), (39) and (40) (Avila *et al.* , 2015; Guerra *et al.* , 2013)

$$C' = -\tau_c R_c \tag{38}$$

$$U_m' = -\tau_{um} R_{um} \tag{39}$$

$$U_s' = -\tau_{us} R_{us} \tag{40}$$

The stabilization term, τ is expressed in the Eqs. (41) (42) and (43), and considers the time step, the corresponding velocity of the phase, the element characteristic length and the

dissipative term: the diffusion coefficient or viscosity, respectively, depending on the considered equation, resulting in, for sediment:

$$\tau_c = \frac{1}{\sqrt{\left(c_1 \frac{2}{\Delta t}\right)^2 + \left(c_2 \frac{\|\mathbf{u}_s\|}{h_{el}}\right)^2 + \left(c_3 \frac{D_s}{h_e l^2}\right)^2}} \tag{41}$$

$$\tau_{um} = \frac{1}{\sqrt{\left(c_1 \frac{2}{\Delta t}\right)^2 + \left(c_2 \frac{\|\mathbf{u}_m\|}{h_{el}}\right)^2 + \left(c_3 \frac{\nu_{eff,m}}{h_e l^2}\right)^2}} \tag{42}$$

$$\tau_{us} = \frac{1}{\sqrt{\left(c_1 \frac{2}{\Delta t}\right)^2 + \left(c_2 \frac{\|\mathbf{u}_s\|}{h_{el}}\right)^2 + \left(c_3 \frac{\nu_s}{h_e l^2}\right)^2}} \tag{43}$$

where the parameter c_1 , c_2 and c_3 are constants and usually choosen as 1, 2 and 4, respectively. An analogous approach is done for the mixture. The residua come from the corresponding governing equations, resulting in Eqs. (44), (45) and (46) for sediment concentration, mixture velocity and sediment velocity, respectively,

$$R_c = \frac{\partial C^h}{\partial t} + W_s \frac{\partial C^h}{\partial z} - \frac{\partial}{\partial z}\left[D_s \frac{\partial C^h}{\partial z}\right] \tag{44}$$

$$R_{one} = \frac{\partial \rho_0 U_m^h}{\partial t} - \frac{\partial}{\partial z}\left[\nu_m \frac{\partial \rho_0 U_m^h}{\partial z}\right] - \rho_m g S \tag{45}$$

$$R_{us} = \frac{\partial C U_s^h}{\partial t} + \frac{\partial C U_s^h W_s}{\partial z} - \frac{\partial}{\partial z}\left[\nu_s \frac{\partial C U_s^h}{\partial z}\right] - C g S - \frac{F_{D,x}}{\rho_s} - \frac{F_{VM,x}}{\rho_s} - \frac{F_{L,x}}{\rho_s} \tag{46}$$

Applying the decomposition, SSTM has a set of six governing equations (15) until (20). Equations (15), (17), (19) and (20) are respected naturally due to the assumptions of the model. It remains only two equations: the sediment transport and the mixture momentum balance, Eqs. (16) and (18) respectively. Applying the RBVMS formulation, it results:

$$\frac{\partial C^h}{\partial t} + \frac{\partial C'}{\partial t} + W_s \frac{\partial C^h}{\partial z} + W_s \frac{\partial C'}{\partial z} - \frac{\partial}{\partial z}\left(D_s \frac{\partial C^h}{\partial z}\right) - \frac{\partial}{\partial z}\left(D_s \frac{\partial C'}{\partial z}\right) = 0 \tag{47}$$

and

$$\frac{\partial \rho_0 U_m^h}{\partial t} + \frac{\partial \rho_0 U_m'}{\partial t} - \frac{\partial}{\partial z}\left(\nu_m \frac{\partial \rho_0 U_m^h}{\partial z}\right) - \frac{\partial}{\partial z}\left(\nu_m \frac{\partial \rho_0 U_m'}{\partial z}\right) - \rho_m g S = 0 \tag{48}$$

where only the buoyancy force is considered. The terms of the subgrid derivatives in time are disregarded, as in (Guerra *et al.* , 2013; Avila *et al.* , 2015; Bauer *et al.* , 2012; Avila *et al.* , 2014). The equation (48) affects the concentration force term, both coarse and fine scales, through the mixture properties rules (Eq. (9)).

For PTFM, represented by the set of six equations (21) until (20), both the mixture momentum balance equation and the sediment mass balance are analogous to the SSTM formulation

shown, differing only in the variable consideration, accordingly to the governing equations. The additional equation is the Eq. (49), the sediment momentum balance,

$$\begin{aligned}\frac{\partial C\rho_s U_s^h}{\partial t} + \frac{\partial C\rho_s U_s'}{\partial t} + \frac{\partial C\rho_s U_s^h W_s}{\partial z} + \frac{\partial C\rho_s U_s' W_s}{\partial z} \\ -\frac{\partial}{\partial z}\left[\nu_s \frac{\partial C\rho_s U_s^h}{\partial z}\right] - \frac{\partial}{\partial z}\left[\nu_s \frac{\partial C\rho_s U_s'}{\partial z}\right] \\ -C\ rho_s g S - F_{D,x} - F_{MV,x} - F_{L,x} \\ = 0\end{aligned} \tag{49}$$

The velocity subgrid decomposition has not been taken into account in the force terms, which is an approximation. The term $\frac{\partial CU_s'}{\partial t}$ results in unusual RBVMS terms involving the product of the subgrid velocity by the time derivative of concentration. Thus, it brings additional turbulence and transport elements. The forces involved at the time balance depend on, in principle, the subgrid velocities, but it will be considered only concentration subgrid values.

Those equations are solved using a standard Generalized Minimal Residual Algorithm (GMRES) and the Newton's method for marching in time. Each equation is solved independently into an iterative loop until reaching convergence. The framework has the iterative resolution of each equation embedded into a global iterative loop in order to deal with all non-linearities.

3.5 Sensitivity analysis

Looking at the inherent uncertainty of the maximum packing fraction and the exponential parameter of the phenomenological equation it was carried out a stochastic colocation method in order to perform a sensitivity analysis of the exponential parameter. Figure 1 shows that a dispersion of this parameter is a way to embed model uncertainties. This idea is the basis of the stochastic colocation analysis which uses Clenshaw-Curtis quadrature (Nobile *et al.* , 2008; Guerra *et al.* , 2012; Gerstner & Griebel, 1998) and Chebyshev abscissa. The nested sparse grid approach offers the advantage of reusing the solution of each level, very useful when dealing with great amount of data. The abscissa for each level are found using Eq. (50) and weights for each point by the Eq. (51)

$$x_j^i = -\cos\frac{\pi(j-1)}{m_i - 1} \tag{50}$$

for $1 \leq j \leq m_i$ to m_i the number of level points i found by $m_1 = 1$ or $m_i = 2^{i-1} + 1$. The abscissa are calculated for a support $[-1; 1]$ then being transformed to the support of the variable λ considered uniform in $[1, 4; 3, 8]$.

$$w_{(x_j^i)} = \frac{2}{m_i}\left(1 + \sum_{l=1}^{(m_i-1)/2} \frac{1}{2} cos1 - 4l^{\left(\frac{2\pi(i-1)}{m_i-1}\right)}\right) \tag{51}$$

4 RESULTS

In order to understand better physics and evaluation of code implementation, different open channel setups were simulated considering different values of quantities that affect the flow

dynamics: the concentration and the slope of the flow domain. The initial velocity is considered equal in each scenario. The initial flow concentration has constant values in z of 0.1 %; 0.5 % and 1 %. For the slope, three values found in the literature were used: 0.000739; 0.00251 and 0.0113 radians according to the experiments of Lyn (1988), Muste & Patel (1997) as Muste *et al.* (2005) respectively. The phenomenological equation of Krieger and Dougherty was used for SSTM model. This procedure aims to compare the effect of the phenomenological model applied in SSTM with the interaction forces of PTFM, this due to the hierarchy of the physical-mathematical formulation.

Sediment has a constant diameter of 0.21 mm with constant settling velocity of $0.0012m/s$. The initial velocity profile in the direction of flow was considered to be zero in x. The height of the domain is the same order of others papers found in literature, it is 0.2 m (Bombardelli & Jha, 2009; Lyn, 1988; Muste & Patel, 1997; Muste *et al.* , 2005). The time step is $0.01s$ respecting then the pseudo Courant-Friedrich-Leibnitz number calculated as $\frac{\Delta z}{\Delta t} \leq W_{set}$ (Bombardelli & Jha, 2009).

Typically, the iterative sub-processes of the several equations presented convergence around 2 to 7 iterations, with a tolerance of 10^{-6} and this, for different spatial discretizations and setups. Looking at the convergence of the mesh, 100 elements showed to be a good discretization. The mass balance over time was used to evaluate the numerical solution and the normalized mass balance showed an oscillation of amplitude of 10^{-6} around 1, ie there is mass conservation. This occurs for both models, SSTM and PTFM and for different scenarios.

Another quantity that is important do monitorate in the evaluation of the simulation results is energy budget. In this work, only the sum of the potential and kinetic energy was monitored, defined as ξ , Eq. (52), such that

$$k + E_p = \xi \tag{52}$$

where the sum of the kinetic energy k with the potential energy E_p is considered to evaluate the energy dissipation over time. The kinetic energy and potential energy term are found at each time step from the Eqs. (53) and (54), respectively, as shown in Necker *et al.* (2002):

$$k(t) = \int_\Omega \frac{1}{2} \rho_m U_m U_m d\Omega \tag{53}$$

$$E_p(t) = \int_\Omega \rho_s g C z d\Omega \tag{54}$$

where Ω is the domain, $E_p(t)$, the potential energy and $k(t)$, kinetic energy in function of time t. Fig. 3 shows the sum of the two energies for PTFM and SSTM model.

As should be expected, the energy present in the system shows a greater dissipation with the phenomenological model. The result the mixture and concentration velocity presented very similar pattern for both models. As can be seen in Fig. 5 the difference only becomes perceptible in the velocity profile when the viscosity law is applied. This occurs analogously in all considered scenarios.

In concentration profiles, there are no significant differences between models and the same occurs in the different scenarios analyzed. The conclusion that can be made is that the velocity profile is more affected by the slope than by concentration, wich is represented in Fig. 4. The correction of viscosity affects the velocity profile in SSTM model, but it doesn't recover, as expected, the PTFM pattern, Fig. 5.

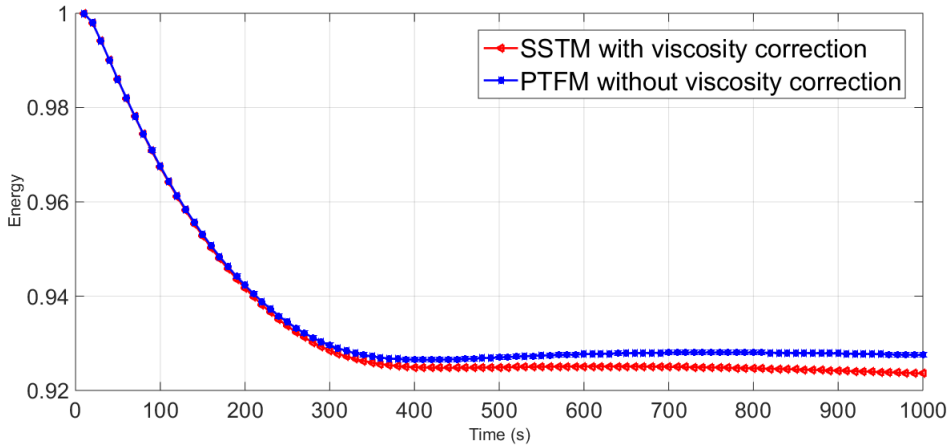

Figure 3: Plot over time of the sum of potential energy and kinetic normalized by the total energy at t = 0.

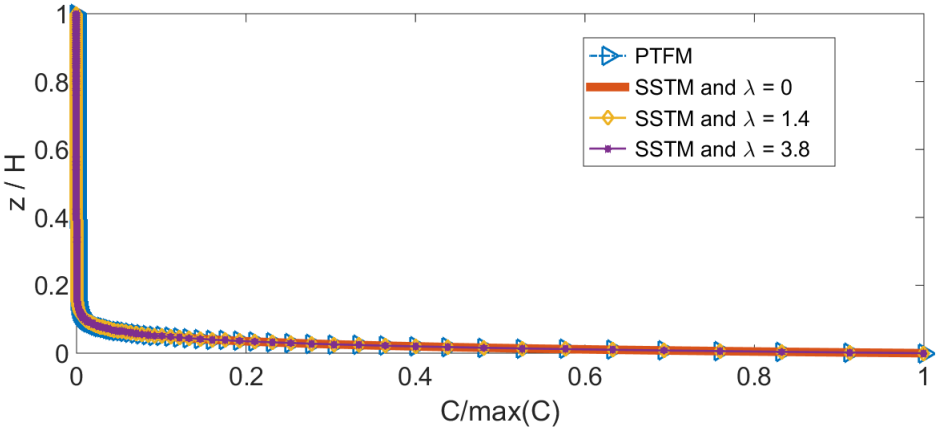

Figure 4: Comparison between models: concentration pattern at final time

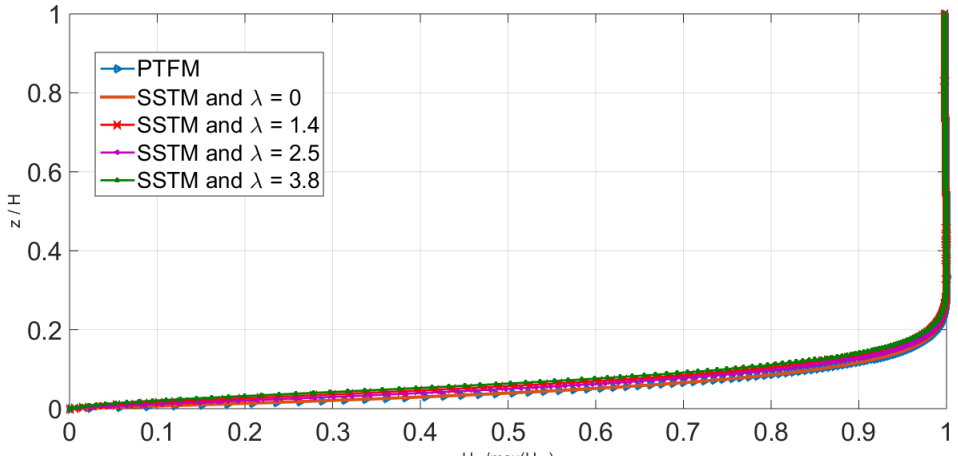

Figure 5: Comparison between models: mixture velocity pattern at final time.

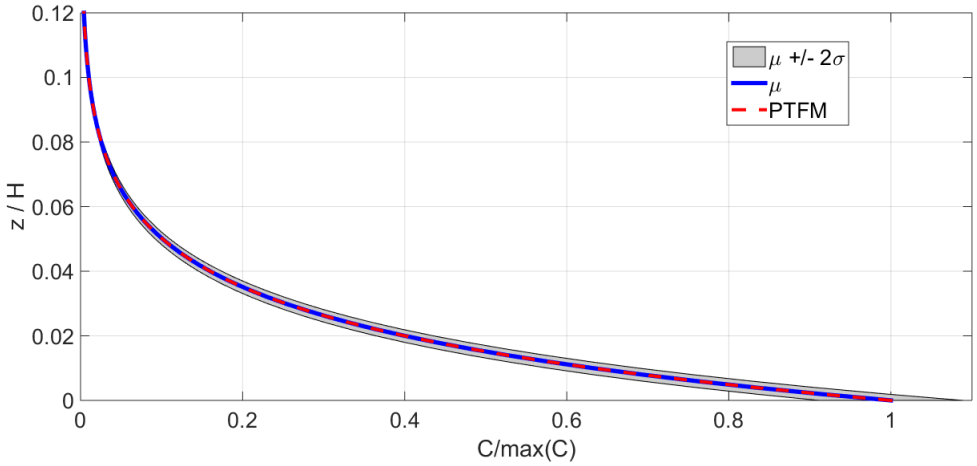

Figure 6: Stochastic SSTM result comparing with concentration profile of PTFM at final time, average +/- 2 standard deviations, with zoom to the area of interest

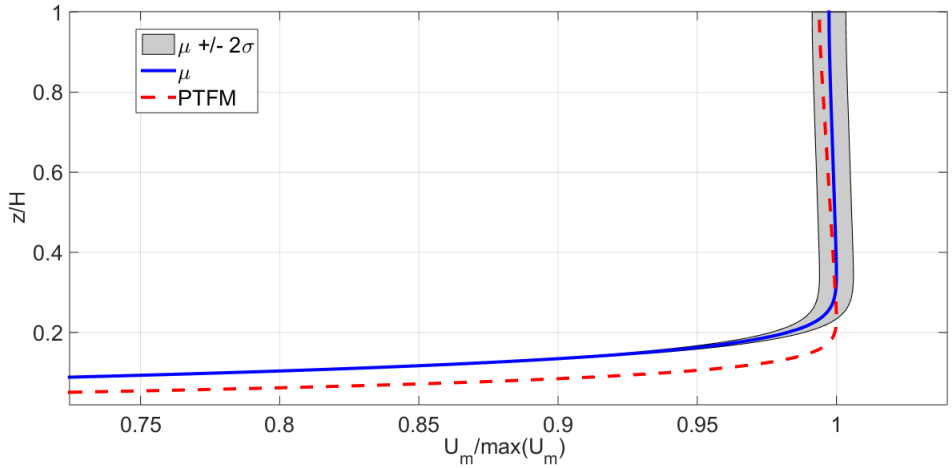

Figure 7: Stochastic result comparing mixture velocity profile of SSTM with PTFM at final time, average +/- 2 standard deviations, with zoom to the area of interest.

To analyze the relationship of interaction forces with the phenomenological models of rheology, a sensitivity analysis of the exponential parameter were performed. In this attempt, the Figures 6 and 7 show the mean and standard deviation found with this procedure on the rheological model applied in SSTM. There, is shown the comparison of the respective profiles with the PTFM solution for the same configuration. Figure 8 explicit the criteria of convergence reached level 8, based on the shear stress of the flow at the bottom.

These preliminary results of the stochastic analysis were not very conclusive because they don't express exactly what would be expected. The region where concentration has more influence, near the bottom, shows a significant deviation of between the velocity mean and the PTFM curve. For the concentration profile, the mean of the colocation procedure is the same that the PTFM. Any solid conclusion can be made at this stage because the complexity of turbidity currents equations and phenomena can affect more than it seems in the sensitivity analysis. However, further investigation on the process as a whole is needed.

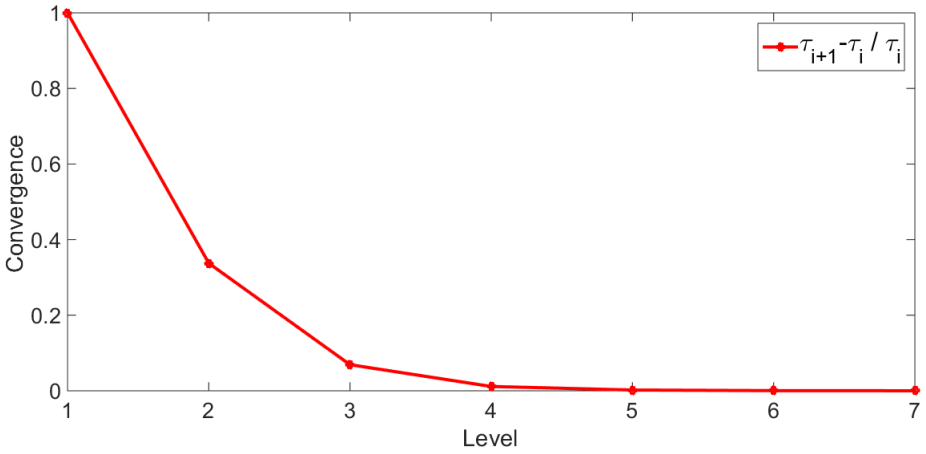

Figure 8: Plot of the convergence criterion evaluated by the shear stress at the bottom

CONCLUSION

The deterministic results are good when compared with literature. Stochastic colocation methods for uncertainty quantification showed to be very helpful even if the complexity of the turbidity current does not allow to reach solids conclusions upon rheological models of turbidity currents, only from the uncertainty quantification point of view taken. However, in this work in progress, which employs the comparison between hierarchical models solved with the subgrid decomposition *Residual Based Variational Multiscale Method* with Finite Element Method is a good indication of how uncertainty quantification may be useful in decision-making regarding the determination of empirical parameters. In the world of turbidity currents, on the analysis of phenomenological models associated therewith, little is found in literature. Existing analyses commonly refer to a certain specific pattern or the comparison of some of them. The continuity of this work is based on the idea that uncertainty quantification is a powerful and reliable tool to unify the different phenomenological models, not only referring to the rheology, but perhaps, also to other phenomena related to the turbidity currents as the sedimentation rate, or even the use of phenomenological laws in extremely dense currents.

REFERENCES

Arrhenius, S. 1917. The Viscosity of Solutions. *Biochemical Journal*, **11**(2), 112–133.

Avila, M., Codina, R., & Principe, J. 2014. Large eddy simulation of low Mach number flows using dynamic and orthogonal subgrid scales. *Computers and Fluids*, **99**(jul), 44–66.

Avila, M., Codina, R., & Principe, J. 2015. Finite element dynamical subgrid-scale model for low Mach number flows with radiative heat transfer. *International Journal of Numerical Methods for Heat and Fluid Flow*, **25**(6), 1361–1384.

Bakhtyar, R., Yeganeh-Bakhtiary, A., Barry, D.A., & Ghaheri, A. 2009. Two-phase hydrodynamic and sediment transport modeling of wave-generated sheet flow. *Advances in Water Resources*, **32**(8), 1267–1283.

Batchelor, G. K. 1977. The effect of Brownian motion on the bulk stress in a suspension of spherical particles. *Journal of Fluid Mechanics*, **83**(01), 97.

Bauer, G., Gravemeier, V., & Wall, W. A. 2012. A stabilized finite element method for the numerical simulation of multi-ion transport in electrochemical systems. *Computer Methods in Applied Mechanics and Engineering*, **223-224**(jun), 199–210.

Bombardelli, F. A., & Jha, S. K. 2009. Hierarchical modeling of the dilute transport of suspended sediment in open channels. *Environmental Fluid Mechanics*, **9**(2), 207–235.

Brady, J. F. 1993. The rheological behavior of concentrated colloidal dispersions. *The Journal of Chemical Physics*, **99**(1), 567.

Brennen, C. E. 2005. *Fundamentals of Multiphase Flows*. Pasadena: Cambridge University Press.

Buscaglia, G. C., Bombardelli, F. A., & García, M. H. 2002. Numerical modeling of large-scale bubble plumes accounting for mass transfer effects. *International Journal of Multiphase Flow*, **28**(11), 1763–1785.

Cao, Z., Wei, L., & Xie, J. 1995. Sediment-Laden Flow in Open Channels from Two-Phase Flow Viewpoint. *Journal of Hydraulic Engineering*, **121**(10), 725–735.

Cao, Z., Egashira, S., & Carling, P. A. 2003. Role of suspended-sediment particle size in modifying velocity profiles in open channel flows. *Water Resources Research*, **39**(2), n/a–n/a.

Chong, J. S., Christiansen, E. B., & Baer, A. D. 1971. Rheology of concentrated suspensions. *Journal of Applied Polymer Science*, **15**(8), 2007–2021.

Dong, P., & Zhang, K. 1999. Two-phase flow modelling of sediment motions in oscillatory sheet flow. *Coastal Engineering*, **36**(2), 87–109.

Einstein, A. 1906. Eine neue Bestimmung der Moleküldimensionen. *Annalen der Physik*, **324**(2), 289–306.

Elghobashi, S. E. 1983. A two-equation turbulence model for two-phase flows. *Physics of Fluids*, **26**(4), 931.

Gerstner, T., & Griebel, M. 1998. Numerical integration using sparse grids. *Numerical Algorithms*, **18**(3/4), 209–232.

Guerra, G., Rochinha, F. A., Elias, R., de Oliveira, D., Ogasawara, E., Dias, J. F., Mattoso, M., & Coutinho, A. L. G. A. 2012. Uncertainty Quantification In Computational Predictive Models For Fluid Dynamics Using A Workflow Management Engine. *International Journal for Uncertainty Quantification*, **2**(1), 53–71.

Guerra, G. M., Zio, S., Camata, J., Rochinha, F. A., Elias, R. N., Paraizo, P. L.B., & Coutinho, A. L.G.A. 2013. Numerical simulation of particle-laden flows by the residual-based variational multiscale method. *International Journal for Numerical Methods in Fluids*, **73**(8), 729–749.

Jha, S. K., & Bombardelli, F. A. 2010. Toward two-phase flow modeling of nondilute sediment transport in open channels. *Journal of Geophysical Research*, **115**(F3), F03015.

Jha, S. K., & Bombardelli, F. A. 2011. Theoretical/numerical model for the transport of non-uniform suspended sediment in open channels. *Advances in Water Resources*, **34**(5), 577–591.

Krieger, I. M., & Dougherty, T. J. 1959. A Mechanism for Non-Newtonian Flow in Suspensions of Rigid Spheres. *Journal of Rheology*, **3**(1), 137.

Lyn, D. A. 1988. A similarity approach to turbulent sediment-laden flows in open channels. *Journal of Fluid Mechanics*, **193**(1), 1.

Mooney, M. 1951. The viscosity of a concentrated suspension of spherical particles. *Journal of Colloid Science*, **6**(2), 162–170.

Muste, M., & Patel, V. C. 1997. Velocity Profiles for Particles and Liquid in Open-Channel Flow with Suspended Sediment. *Journal of Hydraulic Engineering*, **123**(9), 742–751.

Muste, M., Yu, K., Fujita, I., & Ettema, R. 2005. Two-phase versus mixed-flow perspective on suspended sediment transport in turbulent channel flows. *Water Resources Research*, **41**(10).

Necker, F., Härtel, C., Kleiser, L., & Meiburg, E. 2002. High-resolution simulations of particle-driven gravity currents. *International Journal of Multiphase Flow*, **28**, 279–300.

Nobile, F., Tempone, R., & Webster, C. G. 2008. An Anisotropic Sparse Grid Stochastic Collocation Method for Partial Differential Equations with Random Input Data. *SIAM Journal on Numerical Analysis*, **46**, 2411–2442.

Pavlik, M. 2011. *The dependence of suspension viscosity on particle size, shear rate, and solvent viscosity*. Ph.D. thesis, DePaul University.

Roscoe, R. 2002. The viscosity of suspensions of rigid spheres. *British Journal of Applied Physics*, **3**(8), 267–269.

Thomas, D. G. 1965. Transport characteristics of suspension: VIII. A note on the viscosity of Newtonian suspensions of uniform spherical particles. *Journal of Colloid Science*, **20**(3), 267–277.

Toda, K., & Furuse, H. 2006. Extension of Einstein's viscosity equation to that for concentrated dispersions of solutes and particles. *Journal of bioscience and bioengineering*, **102**(6), 524–8.

Widera, P. 2011. *Study of sediment transport processes using Reynolds Averaged Navier-Stokes and Large Eddy Simulation*. Ph.D. thesis, VRIJE UNIVERSITEIT BRUSSEL.

Winterwerp, J.C. 2002. On the flocculation and settling velocity of estuarine mud. *Continental Shelf Research*, **22**(9), 1339–1360.